

# RESEARCH OF THE MECHANISMS OF BACKFILL FORMATION AND DAMAGE

## RAZISKAVA MEHANIZMOV OBLIKOVANJA IN POŠKODOVANJA ZASUTJA

Rugao Gao, Keping Zhou, Jieli Li

Central South University, College of Resources and Safety Engineering, Hunan Changsha 410083, China  
gaorgesu@163.com

*Prejem rokopisa – received: 2017-06-09; sprejem za objavo – accepted for publication: 2017-07-28*

doi:10.17222/mit.2017.070

This work aims to improve the research method relating to the formation and destruction of the mechanical properties of a backfill. The hydration and pore-distribution characteristics of a backfill were examined with an AniMR-150 nuclear-magnetic-resonance instrument and MIRA3 scanning electron microscopy. Microscopic studies show that the porosity change of the backfill tends to be stable after 7 d, and the formation of chemically bound water is the main reason for a dense microstructure of the backfill with a high cement-tailing ratio. Based on the principle of the Lemaitre strain equivalence, non-linear constitutive equations of backfill damage were proposed and validated, revealing the stress-strain characteristics of the process of backfill damage. The work introduces a micro-physical mechanism into the backfill-property analysis, which provides a new scientific basis for the preparation and application of an appropriate design of a frame filling.

Keywords: cemented-tailing backfill, nuclear magnetic resonance, hydration characteristics, mechanical properties

Namen tega dela je izboljšati raziskovalno metodo pri nastajanju in uničevanju mehanskih lastnosti zapolnjevanja. Karakteristike za hidratacijo in porazdelitev por so bile preizkušene z instrumentom za jedrsko magnetno resonanco AniMR-150 in z elektronsko mikroskopijo. Mikroskopske študije kažejo, da je sprememba poroznosti v 7 d stabilna in da je nastanek kemično vezane vode glavni razlog za gosto mikrostrukturo polnila z visokim cementnim razmerjem. Na podlagi principa ekvivalence sevov po Lemaitreu, so bile predlagane in validirane nelinearne konstitutivne enačbe defektov, ki nastanejo pri povratnem polnjenju, kar kaže na značilnosti napetostne sile defektov v zapolnitvenem procesu. Delo uvaja mikrofizikalni mehanizem pri analizi lastnosti samozapolnjevanja, ki omogoča novo znanstveno osnovo za pripravo in aplikacijo ustreznega dizajna in okvirnega polnila.

Ključne besede: cementno polnilo, nuklearno-magnetna resonanca, karakteristike hidratacije, mehanske lastnosti

## 1 INTRODUCTION

Backfill-mining technology plays a significant role in environmental protection and the prevention of water-resource pollution.<sup>1,2</sup> Therefore, it is being widely and intensively employed in the global mining industry. Various types of research on the mechanical properties of the backfills were conducted in order to reduce the ore dilution and loss during pillar robbing. Distinguished by concrete, backfill is a kind of a multiphase composite material with fractures, cracks, bubbles and cavities, and a low intensity. The deformation of a backfill medium is not only due to its brittleness.<sup>3,4</sup> Therefore, research of backfill-material mechanical properties changed from classical-macroscale to mesoscopic-scale research.

In backfill slurry, water is attached to the pores between the material surface and the particles; the molecular movement of the moisture is limited. The limiting effect of solid-pore walls on the surface adsorption of water and the paramagnetic ions on the surface of the cement particles can lead to additional surface-relaxation mechanisms. The distribution of the internal pore-bound water hydrogen nuclei in a saturated slurry was carried out with nuclear magnetic resonance. The T2 relaxation

time of the slurry in different curing periods was determined with the CPMG method. The internal microstructural evolution behavior of the backfill was tested with these methods, and the test results were verified with electron microscopy.

Backfills with different cement-tailing ratios were tested to obtain the necessary mechanical parameters and the stress-strain curve. Deformation and failure characteristics of the backfills were analyzed to derive the damage-constitutive equation, then the reliability was validated. Damage analyses of the backfills with different ratios based on the Lemaitre strain equivalent hypothesis were carried out,<sup>5</sup> then a constitutive model of a backfill based on continuum-damage mechanics was established.

## 2 EXPERIMENTAL PART

### 2.1 Hardening test of the filling slurry based on nuclear magnetic resonance

Backfilling slurries with cement-tailing ratios of 0.333:1, 0.200:1 and 0.125:1 were compounded of unclassified tailings and 325# Portland cement. An electronic balance with an accuracy of 0.01 g was used

for weighing. During the stirring process, the cement and the tailings were mixed uniformly and then water was poured into the mixing bucket. Finally, the mixed cement and the tailings were added into the mixing bucket to be stirred for 10 min. After the mixing, the prepared filling-slurry samples were put into an AniMR-150 nuclear-magnetic-resonance instrument for a CPMG test, with the probe-coil diameter being 15 mm. The room temperature of the test was adjusted to 26 °C using air conditioning.

In the CPMG experiment, the transverse relaxation time (T2) was collected for the first time 5 min after the start of the stirring with water, and the T2 data was collected at intervals.

The early hydration of Portland cement took place about 3 h after the water addition, so the total time for all the signals collected was controlled within 200 min.

**2.2 Mechanical test of the cemented-tailing backfills**

Backfill specimens with cement-tailing ratios of 0.250:1, 0.167:0, 0.125:1, 0.100:1 and 0.083:1 were compounded of classified tailings and 325 # Portland cement (five pieces per group). The specimens were cut into 70-mm cubes with an unevenness of the bearing surface of not more than 0.05 mm per 100 mm. After being kept in a curing room for 28 d and at 26 °C, the specimens were subjected to a uniaxial compression test with an electro-hydraulic servo-testing machine.

**3 RESULTS AND DISCUSSION**

**3.1 Formation characteristics of the cemented-tailing backfill**

The spin-echo series recorded by the CPMG sequence (transverse relaxation measurement) is not the attenuation of a single T2 value, but the distribution of T2 values. The relationship between different levels of porosity in a porous medium and the spin-echo series are shown in **Figure 2**.

The distribution of the T2 spectrum during the hardening process of the filling slurries with different cement-tailing ratios are shown in **Figure 3**. It can be

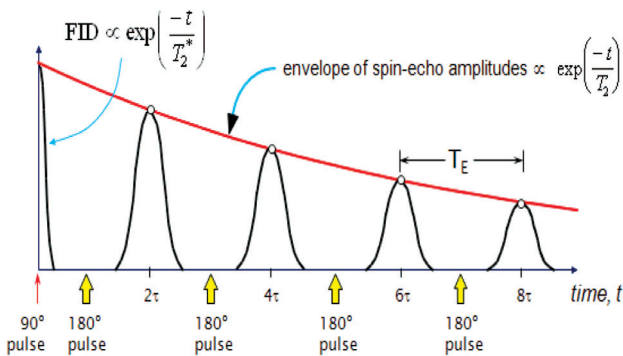


**Figure 1:** CPMG sequence

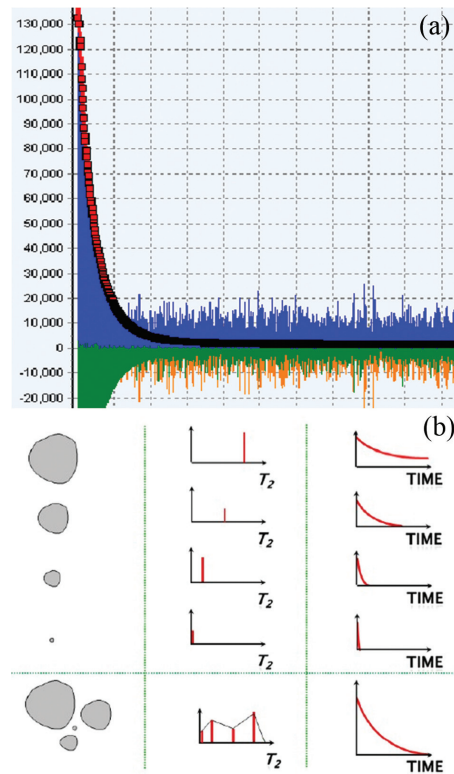


**Figure 2:** Magnetic resonance monitoring: a) peak decay curve of CPMG signal, b) correspondence between the attenuation of spin echoes and the distribution of porosity in porous media

seen from the figure that the T2 distributions of the filling slurries with different ratios contain one main peak and one or two secondary peaks. The peak area of the main peak occupies more than 96 %. The T2 distributions of the filling slurries with different ratios are mainly concentrated at 0.2-10 ms.

With the hydration reaction proceeding, the T2 distributions of the three kinds of backfilling slurry move to the left. The left-shift speed of the filling slurry is relatively fast; after 3–7 d, the left-shift speed is relatively slow; after 7 d, the distribution of the main-peak area and T2 value of the filling slurry is very slow and the left-shift phenomenon is not obvious. The leftward-shift velocity of the T2 distribution of the filling slurry can reflect the hydration-reaction rate in the filling slurry. The displacement of T2 showed that the hydration rate was the fastest in the first three days and it decreased from the third day to the seventh day as the hydration reaction proceeded slowly.

The weighted average T2-weighted values of the slurries with cement-tailing ratios of 0.333:1, 0.200:1 and 0.125:1 were (3.51, 4.04 and 4.64) ms, respectively. The 0.200:1 and 0.125:1 filled slurries had weighted average pore sizes of 1.15 times and 1.32 times the weighted average pore diameter of the 0.333:1 filled slurry. After 3 d, the weighted average T2 main peaks of 0.333:1, 0.200:1 and 0.125:1 were (1.75, 2.01 and 3.05) ms, respectively. The 0.200:1 and 0.125:1 filled slurries had weighted average pore sizes of 1.15 and 1.74 times

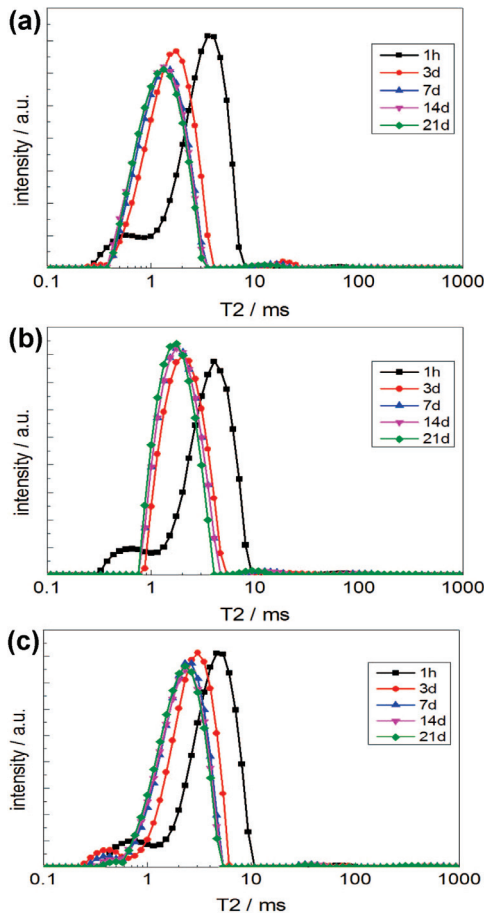


**Figure 3:** T2 spectrum characteristics of backfills with different ratios at different ages: a) sample with a cement-tailing ratio of 0.333:1, b) sample with a cement-tailing ratio of 0.200:1, c) sample with a cement-tailing ratio of 0.125:1

the weighted average pore size of the 0.333:1 filled slurry. After 7 d, the weighted average T2 value of the main peak of the filling slurry with a different ratio of lime to sand tended to be stable. The weighted average T2 values of the main peaks of the filling slurry were 1.32, 1.75 and 2.31 ms after 21 d, respectively. The 0.200:1 and 0.125:1 filled slurries had weighted average

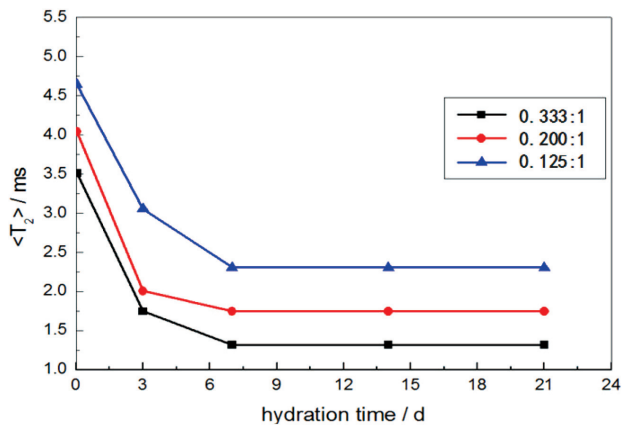


**Figure 4:** Weighted average T2 main-peak value of the filling slurry with a different cement-tailing ratio

pore sizes of 1.33 and 1.75 times the weighted average pore diameter of the 0.333:1 filled slurry.

As shown in **Figure 4**, the higher the filling-slurry ratio, the smaller is the T2 peak value, which means that the higher the cement-tailing ratio, the smaller is the overall pore size of the backfilling slurry. With a different cement-tailing ratio, the amount of hydration product is different and so is the original pore density of the backfill. The higher the proportion of the backfilling slurry, the more hydration products there are, resulting in more tailings, a decreased filling-slurry porosity and pore diameter, and a good hardening effect.

When the  $\text{Ca}^{2+}$  ion component in the cement is substantially converted to  $\text{Ca}(\text{OH})_2$  and equilibrated, the slurry loses its fluidity and changes from viscoplastic to

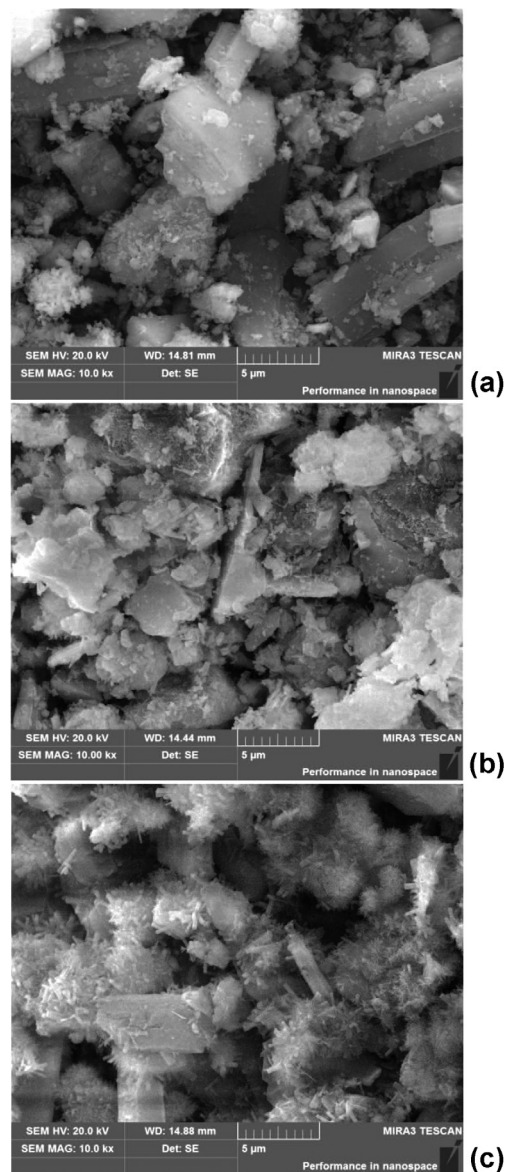


**Figure 5:** Electron-microscopy images of the slurry cured for 7 d: a) sample with a cement-tailing ratio of 0.125:1, b) sample with a cement-tailing ratio of 0.200:1, c) sample with a cement-tailing ratio of 0.333:1

viscoelastic. The tailings are attacked by alkaline brackets, in which silicate anions and  $Ca^{2+}$  start to form a C-S-H gel (hydrated calcium silicate) on the surfaces of the particles. It can be seen from **Figure 5** that in the case of a higher cement-tailing ratio, the whole tailing is filled with more needle-like C-S-H gel volume, forming a compact structure and resulting in a higher backfill strength. The scanned images validate the accuracy of the NMR test. The main water absorption by the filling slurry takes place during the first seven days; in this period, the porosity is significantly reduced with the increased bleeding and drainage work needs to be done.

### 3.2 Damage characteristics of the cement-tailing backfill

A deformation and failure process involving a cement backfill under uniaxial loading can be divided into four stages according to the stress-strain curves obtained from the experiment (**Figure 6**):

Stage 1: Initial deformation stage (curve *OA* section in **Figure 6**). The compression of fissures occurs inside the specimen.

Stage 2: Linear deformation stage (curve *AB* section in **Figure 6**). The curve is approximately a straight line; the curve of the backfill with a larger elastic modulus is steeper.

Stage 3: Yield stage (curve *BC* section in **Figure 6**). Stress grows slowly and eventually reaches the peak; the higher the cement-tailing ratio, the more distinct is the yielding process of deformation and the higher is the yielding stress.

Stage 4: Failure stage (curve *CD* section in **Figure 6**). The stress value declines gradually and cracks occur in the specimen; the compressive capacity of the backfill is rapidly reduced.

To summarize from the stress and strain regularity, it is evident that the peak stress of backfill is reduced with the cement-tailing ratio, while the strength variation

tends towards stability when the ratio is reduced to a certain extent; after the peak stress, the lower the cement-tailing ratio, the smaller is the deformation and the more abrupt is the occurrence of failure.

### 3.3 Damage-constitutive equations of backfills with different cement-tailing ratios

As the main basis of describing mechanical-property changes, the backfill damage degradation is divided into three stages: deformation, damage and fracture. Macroscopic fractures of backfills are caused by an internal damage accumulation, so the deformation can be primarily analyzed with the constitutive-relation research of damage evolution. According to the principle of Lemaitre's strain equivalence, it can be concluded that when the backfill is regarded as an isotropic continuum<sup>6</sup>

$$\sigma = E\varepsilon(1-D) \tag{1}$$

where  $\sigma$  is the effective stress;  $E$  is the elastic modulus;  $\varepsilon$  is the strain;  $D$  is the damage value.

When  $D = 0$ , the backfill is in no-damage state; when  $D = 1$ , the backfill is in the course of absolute damage or failure.

Loland derived a stress-strain curve containing a damage variable based on the strain-equivalence principle; he deduced damage law by assuming the equation of the expressions of effective stress and strain:<sup>7</sup>

$$D = D_0 + C\varepsilon^\beta \tag{2}$$

where  $D$  is the damage value;  $D_0$  is the initial damage value;  $C$  and  $\beta$  are undetermined constants.

Loland's model assumed a linear relationship between the effective stress and strain; however, as the effective stress is a constant value, it does not change with the strain. There are differences between an assumption and engineering practice. The micro-unit strength of materials obeys the Weibull distribution of the statistical-damage theory, where a damage variable is the probability-density cumulative-distribution function of the material fracture strength. The statistical-distribution equation of damage parameters was determined as the fracture strength of backfills and analyzed in accordance with the Weibull distribution:

$$D = 1 - \psi = 1 - \exp\left[-\left(\frac{\varepsilon}{n}\right)^m\right] \tag{3}$$

where  $m$  is the shape parameter of the Weibull distribution;  $n$  is the scale parameter ( $m, n \geq 0$ ).

Inserting Equation (3) into Equation (1), Equation (1) can be written in the following form:

$$\sigma = E\varepsilon(1-D) = E\varepsilon\left[1 - \exp\left[-\left(\frac{\varepsilon}{n}\right)^m\right]\right] \tag{4}$$

Taking the derivative of  $\varepsilon$  from Equation (1), according to the boundary conditions based on the experiment results, Equation (5) can be derived:

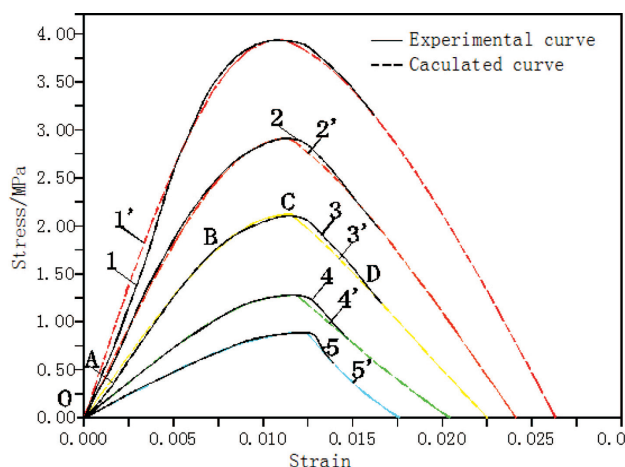


**Figure 6:** Compressive stress-strain curves for the backfill (real lines 1, 2, 3, 4 and 5 stand for cement-tailing ratios of 0.250:1, 0.167:1, 0.125:1, 0.100:1 and 0.083:1, respectively)

$$0 = E\varepsilon \exp\left[-\left(\frac{\varepsilon_p}{n}\right)^m\right] \left[1 - m\left(\frac{\varepsilon_p}{n}\right)^m\right] \quad (5)$$

Equation (5) is used only if

$$1 - m\left(\frac{\varepsilon_p}{n}\right)^m = 0$$

then the scale parameter of the Weibull distribution can be written in the following form:

$$n = \frac{\varepsilon_p}{(1/m)^{1/m}} \quad (6)$$

Inserting Equation (6) into Equation (3), we can describe the damage value  $D$  as:

$$D = 1 - \exp\left[-\frac{1}{m}\left(\frac{\varepsilon}{\varepsilon_p}\right)^m\right] \quad (7)$$

Before the peak stress, the damage-constitutive equation of the backfills under uniaxial loading can be written as:

$$\sigma = E\varepsilon \cdot \exp\left[-\frac{1}{m}\left(\frac{\varepsilon}{\varepsilon_p}\right)^m\right] \quad (8)$$

After the peak stress, where  $\varepsilon_p < \varepsilon \leq \varepsilon_u$  ( $\varepsilon_u$  is the ultimate strain), the stress-strain relationship coincides with the Mazars model of concrete, in which the stress drops exponentially with the increase in the strain. This description fits well with the elastic damage of the backfill under uniaxial test conditions. Therefore, at this stage, the damage value  $D$  is described as:

$$D = D_p + 1 - \exp[-B(\varepsilon - \varepsilon_p)] \quad (9)$$

where  $D_p$  is the damage value when the stress reaches its peak value ( $D_p = 1 - \exp(-1/m)$ ) and  $B$  is the damage parameter of the backfill.

Combining Equation (1) with Equation (9), the damage-constitutive equation of the backfill after the peak stress can be described as:

$$\sigma = -ED_p\varepsilon + E\varepsilon \exp[-B(\varepsilon - \varepsilon_p)] \quad (10)$$

Inserting the results obtained with the experiment such as the stress-strain curves, elastic modulus and peak

**Table 1:** Damage parameter for different backfills

Cement-tailing ratio	Elastic modulus (E/MPa)	Peak stress ( $\sigma_p$ /MPa)	Strain at peak stress ( $\varepsilon_p$ )	Damage at peak stress ( $D_p$ )	Damage parameter		
					( $m$ )	( $1/m$ )	( $B$ )
0.250:1	565	3.95	0.0109	0.3592	2.2473	0.4450	66.49
0.167:1	384	2.92	0.0114	0.3341	2.4593	0.4066	86.32
0.125:1	263	2.13	0.0115	0.2963	2.8457	0.3514	110.58
0.100:1	151	1.29	0.0118	0.2776	3.0749	0.3252	149.01
0.083:1	98	0.89	0.0124	0.2659	3.2351	0.3091	254.74

**Table 2:** Damage-constitutive equations for different backfills

Cement-tailing ratio	Damage-constitutive equation	
	Before the peak stress	After the peak stress
0.250:1	$\varepsilon \leq 0.0109$ $\sigma = 565\varepsilon \left\{ \exp\left[-0.4450\left(\frac{\varepsilon}{0.0109}\right)^{2.2473}\right] \right\}$	$\varepsilon \geq 0.0109$ $\sigma = 565\varepsilon \left\{ -0.3592 + \exp[-66.49(\varepsilon - 0.0109)] \right\}$
0.167:1	$\varepsilon \leq 0.0114$ $\sigma = 384\varepsilon \left\{ \exp\left[-0.4066\left(\frac{\varepsilon}{0.0114}\right)^{2.4593}\right] \right\}$	$\varepsilon \geq 0.0114$ $\sigma = 384\varepsilon \left\{ -0.3341 + \exp[-86.32(\varepsilon - 0.0114)] \right\}$
0.125:1	$\varepsilon \leq 0.0115$ $\sigma = 263\varepsilon \left\{ \exp\left[-0.3514\left(\frac{\varepsilon}{0.0115}\right)^{2.8457}\right] \right\}$	$\varepsilon \geq 0.0115$ $\sigma = 263\varepsilon \left\{ -0.2963 + \exp[-110.58(\varepsilon - 0.0115)] \right\}$
0.100:1	$\varepsilon \leq 0.0118$ $\sigma = 151\varepsilon \left\{ \exp\left[-0.3252\left(\frac{\varepsilon}{0.0118}\right)^{3.0749}\right] \right\}$	$\varepsilon \geq 0.0118$ $\sigma = 151\varepsilon \left\{ -0.2776 + \exp[-149.01(\varepsilon - 0.0118)] \right\}$
0.083:1	$\varepsilon \leq 0.0124$ $\sigma = 98\varepsilon \left\{ \exp\left[-0.3091\left(\frac{\varepsilon}{0.0124}\right)^{3.2351}\right] \right\}$	$\varepsilon \geq 0.0124$ $\sigma = 98\varepsilon \left\{ -0.2659 + \exp[-254.74(\varepsilon - 0.0124)] \right\}$

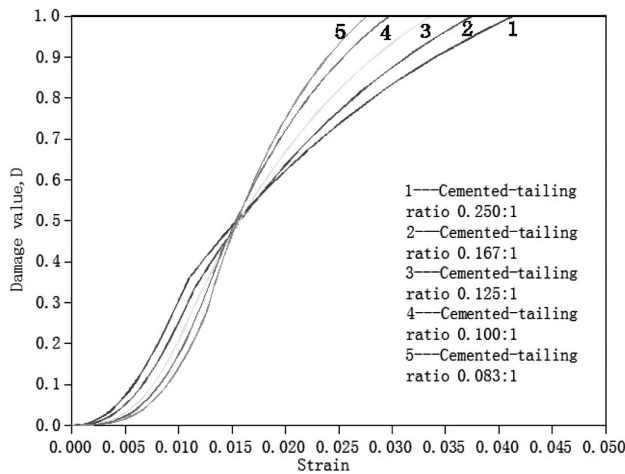


Figure 7: Relationship between damage value ( $D$ ) and strain

strain into Equation (1) and Equation (8), we can obtain the values of  $m$ :

$$m = 1 / \ln \left( \frac{E \varepsilon_p}{\sigma_p} \right) \quad (11)$$

We can also obtain boundary conditions from the theoretical curve speculation and experiment results:

$$\begin{cases} \sigma|_{\varepsilon=\varepsilon_p} = \sigma_p \\ d\sigma / d\varepsilon|_{\varepsilon=\varepsilon_p} = 0 \\ D|_{\varepsilon=\varepsilon_p} = 1 \end{cases} \quad (12)$$

When solving Equation (12), we have:

$$B = -\ln D_p / (\varepsilon_u - \varepsilon_p) \quad (13)$$

Based on the experimental data and solutions of Equation (11) and Equation (13), we can obtain the damage parameters (Table 1) and damage-constitutive equations (Table 2) for different backfills.

By calculating these equations, we can obtain the stress-strain curves of the backfills with different ratios (dashed lines of Figure 6). Compared with the experimental curves, the calculated results agree well with the experimental data.

It is clearly observed from Table 1 that the damage values for different backfills range from 0.26 to 0.35 as the stress reaches its peak. The damage-strain curves of the backfills with different ratios of 0.250:1, 0.167:1, 0.125:1, 0.100:1 and 0.083:1 can be traced with the calculations of the damage-constitutive equations (Figure 7). In Figure 7, we can see that the damage-growth rate reaches its maximum at the peak stress, and that the lower the cement-tailing ratio, the more slightly the damage value increases. However, after the peak stress, the damage values go up steeply with the increase in the strain and the damage values get increasingly large with a decreasing ratio.

The damage-constitutive model established in this paper is in good agreement with the measured full stress-strain curve, which can be used to fit the tensile curve. It is shown that the established damage-constitutive model is reliable and has a certain reference value for engineering.

## 4 CONCLUSIONS

- 1) The process of hydration and pore evolution during the hardening process of a filling slurry is complex, and its dynamic evolution cannot be studied with conventional detection methods. NMR allows an extraordinary method as it has unique non-destructive and non-disruptive features such as dynamic observation of the filling-slurry hydration and pore evolution.
- 2) The filling-slurry hydration is mainly observed in the first seven days, which is an important period for drainage in the project. The effect of a high slurry cementation is more obvious with a lower porosity and a more compact structure. The results show that the effect of the chemical bonding with water has a significant impact on the solidification of the filling.
- 3) From the perspective of damage rules, the damage rate of a backfill reaches its peak at the peak stress. The higher the cement-tailing ratio, the larger is the damage value before the stress reaches its peak. By contrast, the deformation becomes increasingly large after the peak stress. The theoretical curve simulated by the constitutive equation is in good agreement with the experimental curve, and the model can describe the uniaxial compression damage of backfills with different cement-tailing ratios.
- 4) This paper was written based on laboratory experiments and theoretical modeling; the results and achievements can be accurately used in a backfill design and production. This method can reduce the dependence on large-scale experiments and industrial verification, and it also provides for reference values supporting underground mining. Based on further development of the software language, a combination of a numerical simulation and experiments is feasible. These methods will allow us to analyze the paste filling and coarse-aggregate filling on the microscopic scale. Further research is expected to allow more possibilities for backfilling transportation.

## Acknowledgments

The authors would like to acknowledge that the work was supported by the National Natural Science Foundation of China (grant no. 51474252).

### Conflict of interests

The authors declare that there is no conflict of interests regarding the publication of this paper.

### 5 REFERENCES

- <sup>1</sup> Q. Zhang, J. Cui, J. Zheng, X. Wang, Wear mechanism and serious wear position of casing pipe in vertical backfill drill-hole, *Transactions of Nonferrous Metals Society of China*, 21 (2011) 11, 2503–2507, doi:10.1016/S1003-6326(11)61042-X
- <sup>2</sup> T. Belem, M. Benzaazoua, Design and application of underground mine paste backfill technology, *Geotechnical and Geological Engineering*, 26 (2008) 2, 147–174, doi:10.1007/s10706-007-9154-3
- <sup>3</sup> A. Tariq, E. K. Yanful, A review of binders used in cemented paste tailings for underground and surface disposal practices, *Journal of Environmental Management*, 131 (2013) 1, 138–149, doi:10.1016/j.jenvman.2013.09.039
- <sup>4</sup> S. Yin, A. Wu, K. Hu, Y. Wang, Y. Zhang, The effect of solid components on the rheological and mechanical properties of cemented paste backfill, *Minerals Engineering*, 35 (2012) 1, 61–66, doi:10.1016/j.mineng.2012.04.008
- <sup>5</sup> J. Lemaitre, How to use damage mechanics, *Nuclear engineering and design*, 80 (1984) 3, 233–245, doi:10.1016/0029-5493(84)90169-9
- <sup>6</sup> J. Lemaitre, A continuous damage mechanics model for ductile fracture, *Journal of Engineering Materials and Technology*, 107 (1985) 1, 83–89, doi:10.1115/1.3225775
- <sup>7</sup> K. E. Loland, Continuous damage model for load-response estimation of concrete, *Cement and Concrete Research*, 10 (1980) 3, 395–462, doi:10.1016/0008-8846(80)90115-5